Tissue-specific tumor suppressor activity of retinoblastoma gene homologs *p107* and *p130*

Jan-Hermen Dannenberg,[1] Leontine Schuijff, Marleen Dekker, Martin van der Valk, and Hein te Riele[2]

Division of Molecular Biology, The Netherlands Cancer Institute, Plesmanlaan 121, 1066 CX Amsterdam, The Netherlands

The retinoblastoma gene family consists of three genes: *RB*, *p107*, and *p130*. While loss of pRB causes retinoblastoma in humans and pituitary gland tumors in mice, tumorigenesis in other tissues may be suppressed by p107 and p130. To test this hypothesis, we have generated chimeric mice from embryonic stem cells carrying compound loss-of-function mutations in the *Rb* gene family. We found that *Rb/p107*- and *Rb/p130*-deficient mice were highly cancer prone. We conclude that in a variety of tissues tumor development by loss of pRB is suppressed by its homologs p107 and p130. The redundancy of the retinoblastoma proteins in vivo is reflected by the behavior of *Rb*-family-defective mouse embryonic fibroblasts in vitro.

[*Keywords*: Retinoblastoma; cancer; mouse model; pocket proteins]

Supplemental material is available at http://www.genesdev.org.

Received September 10, 2003 revised version accepted September 15, 2004.

Inactivation of the retinoblastoma suppressor pRB has been found in many human cancers, including hereditary retinoblastoma and sporadic breast, bladder, prostate, and small cell lung carcinoma (Friend et al. 1986, 1987; Harbour et al. 1988; Lee et al. 1988; T'Ang et al. 1988; Bookstein et al. 1990). pRB controls the G_1/S transition of the cell cycle by modulating the activity of E2F transcription factors. Hypophosphorylated pRB binds to E2Fs and forms complexes harboring chromatin remodeling proteins like histone deacetylases, SWI/SNF and histone methyltransferases, which actively repress genes that are essential for cell cycle regulation, DNA replication, DNA repair, G_2/M checkpoints and differentiation (Harbour and Dean 2000; Muller et al. 2001; Ishida et al. 2001; Kalma et al. 2001; Rayman et al. 2002; Ren et al. 2002). Upon sequential phosphorylation by Cyclin D/CDK4 and Cyclin E/CDK2 kinases, pRB undergoes a conformational change leading to the release of E2Fs. Derepression and activation of E2F target genes then allows cell cycle progression (Trimarchi and Lees 2002). Conversely, down regulation of Cyclin/CDK activity by the INK4A and CIP/KIP family of cyclin dependent kinase inhibitors (CKI), promotes cell cycle arrest (Ruas and Peters 1998; Sherr and Roberts 1999; Sherr 2001). Thus, inactivation of the G_1/S checkpoint can occur at different levels, and indeed, besides loss of *RB* in many cancers, loss of $p16^{Ink4A}$ function has been found in melanoma, pancreatic, and bladder carcinomas, amplification of *Cyclin D1* in breast, oesophagus, and head-and-neck cancer, and *CDK4* amplification or mutational activation in melanoma (for review, see Sherr 1996).

RB is a member of the retinoblastoma gene family that encodes the so-called pocket proteins pRB, p107, and p130 (Ewen et al. 1991; Hannon et al. 1993; Li et al. 1993; Chow and Dean 1996). All three can repress transcription from E2F-responsive promoters (Zamanian and La 1993; Bremner et al. 1995; Starostik et al. 1996) and are regulated by cell-cycle dependent phosphorylation. (Graña et al. 1998; Lundberg and Weinberg 1998; Canhoto et al. 2000; Hansen et al. 2001). Over-expression of each of the pocket proteins results in growth suppression, although not every (tumor) cell type is equally sensitive to each family member (Zhu et al. 1993; Claudio et al. 1994; Beijersbergen et al. 1995). Whereas pRB predominantly binds E2F1, E2F2, and E2F3, p107 and p130 specifically bind E2F4 and E2F5 (Dyson 1998; Trimarchi and Lees 2002) and each of these complexes appears at different stages of the cell cycle: p130/E2F4 is mainly found in G_0, pRB/E2F in G_0 and G_1, and p107/E2F in S-phase (Dyson 1998). Finally, p107/E2F and p130/E2F complexes act as transcriptional repressors of a set of genes different from that regulated by Rb/E2F complexes (Hurford et al. 1997).

[1]**Present address: Department of Medical Oncology, Dana-Farber Cancer Institute and Department of Medicine and Genetics, Harvard Medical School, Boston, Massachusetts 02115, USA.**
[2]**Corresponding author.**
E-MAIL h.t.riele@nki.nl; FAX 31-20-669-1383
Article and publication are at http://www.genesdev.org/cgi/doi/10.1101/gad.322004.

In primary mouse embryonic fibroblasts (MEFs), pocket proteins collectively regulate the response of cells to growth-inhibiting signals (Dannenberg et al. 2000; Sage et al. 2000). Triple knockout cells were refractory to replicative and oncogenic RAS-induced senescence despite accumulating levels of the cell cycle inhibitors $p16^{INK4A}$, $p19^{ARF}$, p53, and $p21^{CIP}$, indicating that both the $p16^{INK4A}$–Cyclin D/CDK4 and $p19^{ARF}$–MDM2–p53 tumor surveillance pathways converge on the retinoblastoma protein family. By comparing the growth behavior of double knockout MEFs, we now show that p107 and p130 *together* can compensate for loss of pRb in mediating growth arrest following activation of the $p19^{ARF}$–MDM2–p53 pathway.

In mice, homozygous inactivation of *Rb* through the germ-line resulted in embryonic lethality and *Rb* heterozygosity led to development of pituitary gland tumors (Clarke et al. 1992; Jacks et al. 1992; Lee et al. 1992; Wu et al. 2003). In contrast, $p107^{-/-}$ or $p130^{-/-}$ mice in a C57BL/6 background did not show an overt phenotype nor a higher incidence of tumors compared with wild-type mice (Cobrinik et al. 1996; Lee et al. 1996). However, $Rb^{+/-}p107^{-/-}$ and $Rb^{+/-}p130^{-/-}$ mice showed a strongly reduced viability (Lee et al. 1996; J.-H. Dannenberg and H. te Riele, unpubl.).

While these results clearly point to redundant functions of pocket proteins in development, it is unclear whether this also extends to suppression of tumorigenesis. Embryonic lethality associated with pRB deficiency and the reduced viability caused by combinations of knockout alleles of *Rb* gene family members, precludes studying this issue by combining knockout alleles in conventional crosses. Embryonic lethality might be circumvented by using conditional knockout alleles; however, this approach heavily relies on pre-existing knowledge of the spatial and temporal requirements for expression of Cre recombinase. We have therefore taken a more unbiased approach based on our previous observation that embryonic lethality caused by *Rb* deficiency could be circumvented in chimeric mice generated from $Rb^{-/-}$ ES cells (Robanus Maandag et al. 1994). In these animals *Rb*-deficient cells were present in virtually all tissues including the pituitary gland where they developed tumors (Robanus Maandag et al. 1994; Williams et al. 1994a). By this approach we also found that combined inactivation of *Rb* and *p107* resulted in development of retinoblastoma (Robanus Maandag et al. 1998). To explore the role of p107 and p130 in tumor suppression we have generated $Rb^{+/-}p107^{-/-}$, $Rb^{+/-}p130^{-/-}$, and $Rb^{-/-}p130^{-/-}$ chimeras. The broad spectrum of tumors found in these mice but not in pure $Rb^{+/-}$ and chimeric $Rb^{-/-}$ mice identifies both p107 and p130 as tumor suppressors in a variety of different tissues.

Results

Pocket protein requirements for replicative and Ras-induced senescence

We have generated ES cells carrying different combinations of genetically inactivated alleles of *Rb*, *p107*, and *p130* and used these to derive an isogenic set of MEF cultures (Fig. 1A) as described before (Dannenberg et al. 2000). Compared with wild-type MEFs, $Rb^{-/-}$ and $Rb^{-/-}p130^{-/-}$ MEFs showed elevated levels of p107 and $Rb^{-/-}$ and $Rb^{-/-}p107^{-/-}$ MEFs showed up-regulation of p130

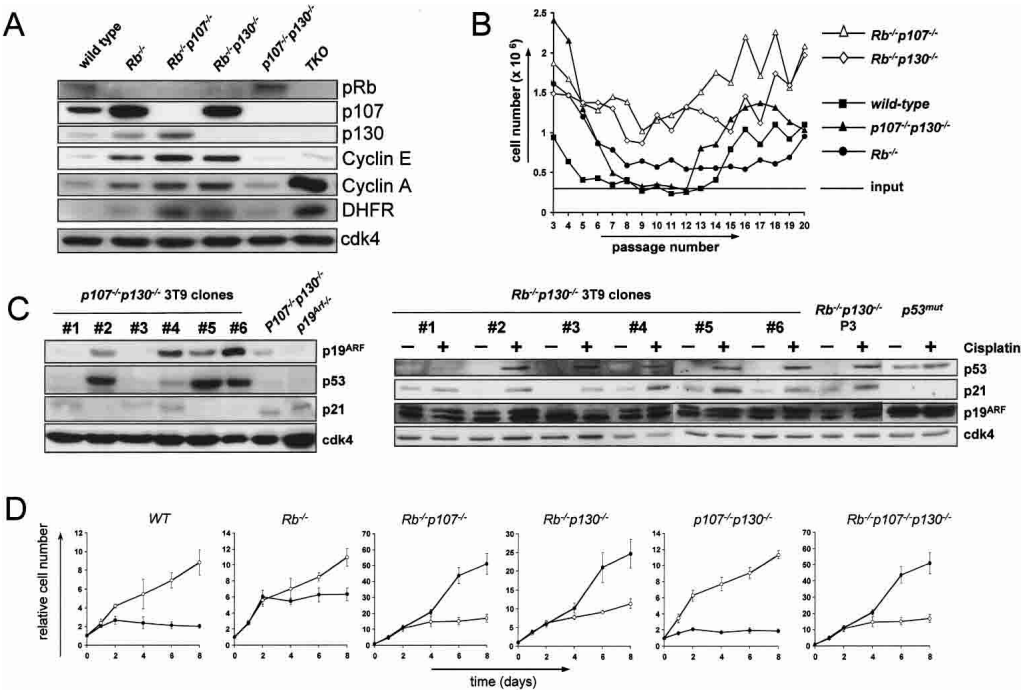

Figure 1. $Rb^{-/-}p107^{-/-}$ and $Rb^{-/-}p130^{-/-}$ MEFs are immortal and resistant to Ras^{V12}-induced senescence. (*A*) Western blot analysis of *Rb*-gene family deficient pMEFs. (*B*) Passaging of pMEFs following a 3T9 protocol shows that $Rb^{-/-}p130^{-/-}$ and $Rb^{-/-}p107^{-/-}$ MEFs are immortal. (*C*) Western blot analysis of $p107^{-/-}p130^{-/-}$ 3T9 clones showing loss of $p19^{ARF}$ expression (clones *1*,*3*) or stabilized mutant p53 (clones *2*,*4*,*5*,*6*). In contrast, $Rb^{-/-}p130^{-/-}$ 3T9 clones show normal $p19^{ARF}$ levels and intact p53 function as evidenced by induction of p21 upon exposure to cisplatin. (*D*) Growth curves of MEFs infected with either control (open circles) or Ras^{V12}-expressing virus (closed circles). Only $Rb^{-/-}p107^{-/-}$, $Rb^{-/-}p130^{-/-}$ and *TKO* MEFs are refractory to Ras^{V12}-induced premature senescence.

(Fig. 1A). Furthermore, both $Rb^{-/-}p107^{-/-}$ and $Rb^{-/-}p130^{-/-}$ MEFs showed increased levels of Cyclin E and A and the E2F1 target DHFR (Fig. 1A). We compared the growth behavior of the three double knockout combinations to that of wild-type and $Rb^{-/-}$ cells. Figure 1B shows that upon serial passaging, wild-type, $Rb^{-/-}$, and $p107^{-/-}p130^{-/-}$ cells rapidly lost proliferative potential and entered a senescent state, albeit that the arrest of $Rb^{-/-}$ cells was somewhat less stringent. In these experiments, all three genotypes escaped senescence after ~13–20 passages. As shown for six $p107^{-/-}p130^{-/-}$ 3T9 clones in Figure 1C, these cells had either lost $p19^{ARF}$ (clones 1,3) or p53 (clones 2,4,5,6). In contrast, $Rb^{-/-}p107^{-/-}$ and $Rb^{-/-}p130^{-/-}$ cells never entered a senescent state but continued to proliferate despite accumulating levels of $p19^{ARF}$ and the presence of active p53 function. Thus, $p19^{ARF}$ was still expressed in six independent $Rb^{-/-}p130^{-/-}$ 3T9 clones obtained from six different MEF isolates (Fig. 1C). Furthermore, treatment of $Rb^{-/-}p130^{-/-}$ 3T9 clones with the DNA damaging agent cisplatin for 24 h induced p53 concomitantly with its target $p21^{CIP}$, indicative for a functional p53 protein (Fig. 1C).

Activation of the $p19^{ARF}$–Mdm2–p53 pathway not only restricts proliferation of cells during prolonged culturing, but also provides a mechanism to block proliferation of cells in the presence of oncogenic signals. Infection of early passage wild-type, $Rb^{-/-}$, $Rb^{-/-}p107^{-/-}$, $Rb^{-/-}p130^{-/-}$, $p107^{-/-}p130^{-/-}$, and *TKO* MEFs with RAS^{V12}-expressing retroviruses resulted in elevated levels of RAS^{V12} and induction of $p19^{ARF}$ and p53 (data not shown). Thus, the pathway normally required by RAS^{V12} to induce a cell cycle arrest was intact in all genotypes. Figure 1D shows that expression of RAS^{V12} suppressed the growth of wild-type and $p107^{-/-}p130^{-/-}$ MEFs and after a brief latency period also of $Rb^{-/-}$ MEFs. In contrast, $Rb^{-/-}p107^{-/-}$ and $Rb^{-/-}p130^{-/-}$ cells were resistant to RAS^{V12}-induced cell cycle arrest and, similar to triple knockout MEFs, showed increased proliferative capacity.

Together with our previous observations (Dannenberg et al. 2000), these results define the minimal requirement for pocket proteins in the $p19^{ARF}$–Mdm2–p53 growth suppression pathway. In particular, p107 *plus* p130 can substitute for loss of pRb to suppress proliferation of MEFs in the presence of oncogenic signaling. These results prompted us to study whether p107 and p130 can also substitute for loss of pRb in suppressing proliferation in vivo.

$Rb^{+/-}p107^{-/-}$ *chimeric mice develop a wide spectrum of tumors*

In pure $Rb^{+/-}$ and chimeric $Rb^{-/-}$ mice, tumor development is restricted to the intermediate lobe of the pituitary gland (Robanus Maandag et al. 1994; Williams et al. 1994a). To study whether tumor development in other tissues was suppressed by p107, we have generated chimeric mice from $Rb^{+/-}p107^{-/-}$ and $Rb^{-/-}p107^{-/-}$ ES cells. The latter genotype resulted in development of retinoblastoma at early age; however, the poor viability of these mice precluded the assessment of tumor susceptibility later in life (Robanus-Maandag et al. 1998). In contrast, $Rb^{+/-}p107^{-/-}$ chimeras were readily obtained and showed high ES cell contribution despite the poor viability of pure $Rb^{+/-}p107^{-/-}$ mice (Lee et al. 1996; J.-H. Dannenberg and H. te Riele, unpubl.).

In a cohort of 53 $Rb^{+/-}p107^{-/-}$ chimeric mice, tumors started to develop after 6 mo, most frequently in the pituitary gland, the coecum, the bone, and lymphoid tissue (Table 1). Primary and metastasized osteosarcoma and leiomyosarcoma are shown in Figure 2A–D. These animals did not develop retinoblastoma but occasionally showed retinal dysplasia (data not shown). A polymorphism in the *Rb* allele allowed us to distinguish by Southern blotting the wild-type *Rb* alleles in blastocyst (C57BL/6)- and ES cell (129OLA)-derived DNA as well as the *Rb* knockout allele. This showed that all tumors were of ES cell origin and that loss of the wild-type *Rb* allele had occurred in all pituitary gland tumors and in 70% of the other tumors (Fig. 2E; Table 1). We conclude that the limited tumor spectrum in *Rb*-deficient mice is caused by tumor suppressor activity of p107 in a variety of tissues.

Tumorigenesis in Rbp130-*deficient chimeras*

To investigate whether p130 can also compensate for loss of pRB in tumor suppression, we followed cohorts of $Rb^{+/-}p130^{-/-}$ and $Rb^{-/-}p130^{-/-}$ chimeric mice. Both genotypes were readily obtained (e.g., $Rb^{-/-}p130^{-/-}$ chimeras at a frequency of 11 out of 28 births as opposed to only seven $Rb^{-/-}p107^{-/-}$ chimeras out of 56 births; Robanus-Maandag et al. 1998). In 15 $Rb^{+/-}p130^{-/-}$ chimeras, we found a thymoma, a hepatoma, a Leydig cell tumor, an insulinoma, and an adrenal gland tumor. However, none of these tumors was found in more than one animal. In contrast, $Rb^{-/-}p130^{-/-}$ chimeric mice consistently developed retinoblastoma, pheochromocytoma, and hyperplasia of neuro-endocrine epithelial cells of the

Table 1. *Tumor incidence in 53* $Rb^{+/-}p107^{-/-}$ *chimeric mice and frequency of* Rb *LOH*

Tumor	Number	Loss of Rb^+ allele[a]
pituitary gland tumor	22	20/20
adenocarcinoma coecum	8	4/6
osteosarcoma	8	3/5
lymphosarcoma	8	4/5
leiomyosarcoma	4	1/1
thymoma	3	0/3
ovary tumor	2	2/2
thyroid tumor	2	1/1
adrenal gland tumor	2	1/1
intestinal tumor	2	1/1
lung tumor	1	1/1
testis tumor	1	1/1
Total	41	20/28

[a]Number of tumors showing loss of the *Rb* wild-type allele/number of tumors tested.

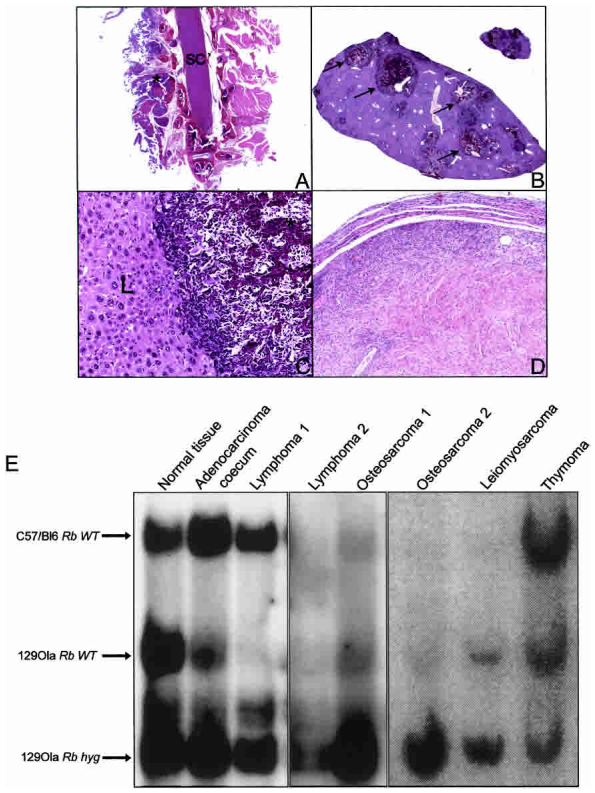

Figure 2. Tumors in $Rb^{+/-}p107^{-/-}$ chimeric mice show *Rb* LOH. Hematoxilyn-eosin-stained histological sections from different tumortypes. (*A*) Osteosarcoma (*) adjacent to the spinal cord (SC). (*B*,*C*) Osteosarcomas often metastasized to the liver (arrows), were associated with large vessels (*B*) and contained osteoid deposits (*C*). (*D*) Leiomyosarcoma located in the uterus. (*E*) Southern blot analysis of tumors using a *Rb*-specific probe. The first lane shows normal tissue showing contribution of the blastocyst-derived Rb^{WT} allele and the ES-derived Rb^{WT} and Rb^{Hyg} alleles. Intestinal adenocarcinomas, osteosarcomas, leiomyosarcomas, and lymphomas but not thymomas, often showed loss of the ES-derived Rb^{WT} allele. The presence of C57/BL6-derived Rb^{WT} DNA in tumors that show loss of the 129OLA Rb^{WT} allele likely results from contaminating tissue. Magnification: *A*,*B*, 2.5×; *C*, 20×; *D*, 5×.

bronchus (Table 2). Probably because of early death of these animals, we did not find pituitary tumors.

Retinoblastoma in $Rb^{-/-}p130^{-/-}$ *chimeric mice*

Retinoblastomas in $Rb^{-/-}p130^{-/-}$ chimeric mice developed at a mean age of 3 mo. The tumors had often filled the posterior eye chamber (Fig. 3A), showed rosette-like structures resembling those in human retinoblastoma (Fig. 3B,C) (Tajima et al. 1994), but had the nuclear morphology of the inner nuclear layer (Fig. 3C,D). Retinoblastomas were found in five out of 11 chimeric animals. Two animals had bilateral and three animals had unilateral retinoblastoma, but one of these had two independent tumors in one eye located at the periphery of the retina (Fig. 3D). In two mice with apparently normal eyes that were sacrificed at 2 wk of age due to tumors at other sites (see below), retinal dysplasia was found in the outer plexiform layer in the peripheral region of the retina. The four remaining animals were poorly chimeric and showed no retinal abnormalities.

To ascertain that the retinoblastomas were of 129OLA ES cell origin, tumor tissue recovered from paraffin sections was subjected to a PCR amplifying the polymorphic CA-repeat sequence D2mit94. 129OLA and C57BL/6 DNA gave 190 and 160 base pair products, respectively. The predominant amplification of a 190 base pair fragment indicates that all three retinoblastomas were of ES cell origin (Fig. 3E).

$Rb^{-/-}p130^{-/-}$ *retinoblastoma has inner nuclear layer characteristics*

Similar to $Rb^{-/-}p107^{-/-}$ retinoblastomas (Robanus-Maandag et al. 1998), we found that $Rb^{-/-}p130^{-/-}$ retinoblastomas did not express IRBP (Fig. 4, cf. A and B,C) but showed positive staining for syntaxin that labels all mature neuronal amacrine cells in the inner nuclear layer and their synaptic processes in the inner plexiform layer (Barnstable et al. 1985) and γ-amino butyric acid (GABA) that identifies GABAergic amacrine cells (Haverkamp and Wässle 2000) (Fig. 4D,H). In most tumors, staining for these two amacrine markers was local (Fig. 4F,J); one early retinoblastoma stained homogeneously for GABA (Fig. 4I). The tumors occasionally showed expression of glutamine synthethase, which identifies Müller glia cells (Bjorklund et al. 1985; Haverkamp and Wässle 2000) and glial fibrillary acidic protein (GFAP), which predominantly recognizes reactive Müller glia cells (Eisenfield et al. 1984) (Fig. 4F–H,J). Finally, the DNA staining pattern of tumor cells closely resembled that of inner nuclear layer cells (Fig. 4E). Thus, both $Rb^{-/-}p130^{-/-}$ and $Rb^{-/-}p107^{-/-}$ retinoblastomas show characteristics of amacrine cells in the inner nuclear layer.

Early stages of $Rb^{-/-}p130^{-/-}$ *retinoblastoma*

To identify early retinal lesions in $Rb^{-/-}p130^{-/-}$ chimeras, we have provided mutant ES cells with a β-galactosidase marker gene, placed under control of the ubiquitously active *Rosa26* promoter (Fig. 5, panel I). X-gal staining of the retina of two 2-wk-old $Rb^{-/-}p130^{-/-}LacZ$ chimeric mice readily identified ES cell-derived hyperplastic lesions in the outer plexiform layer where nor-

Table 2. *Tumor incidence in 11* $Rb^{+/-}p130^{+/-}$ *chimeric mice*

Tumor	Number[a]
retinoblastoma	5
pheochromocytoma	6
lung hyperplasia	7
Total	21

[a]Number of mice showing uni- or bilateral tumors or hyperplasia.

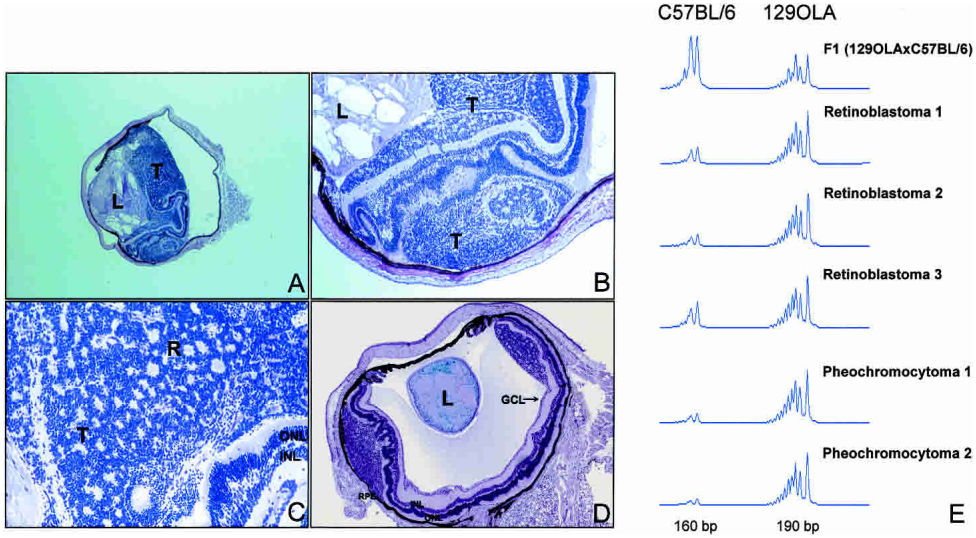

Figure 3. ES cell-derived retinoblastoma in $Rb^{-/-}p130^{-/-}$ chimeric mice. (*A*) Retinoblastoma in a 3-mo-old $Rb^{-/-}p130^{-/-}$ chimera. The lens shows cataracts. (*B*) The tumor has invaded the posterior eye chamber. (*C*,*D*) Rosette-like structures present throughout the tumor. (*D*) Two independent retinoblastomas in the peripheries of the retina in a 1-mo-old $Rb^{-/-}p130^{-/-}$ chimera. One tumor grew between the ONL and the RPE, while the other was growing between the INL and the GCL. (*E*) PCR amplification of the CA-repeat sequence D2Mit94 in DNA from three retinoblastomas (*1–3*) and two pheochromocytomas (*1–2*), giving 190-bp (129OLA) and 160-bp (C57BL/6) fragments. DNA from a F1 (129OLAxC57BL/6) mouse was used as a control. (GCL) Ganglion cell layer; (INL) inner nuclear layer; (L) lens; (ONL) outer nuclear layer; (RPE) retinal pigment epithelium; (R) rosette-like structures; (T) tumor. Magnification: *A*, 2.5×; *B*, 10×; *C*, 20×; *D*, 5×.

mally no nuclei are present (Fig. 5, panel II, A–C). No obvious retinal abnormalities were observed in $Rb^{-/-}p130^{-/-}LacZ$ chimeric embryos at day 18 p.c. (post-coitum) (Fig. 5, panel II, D). The nuclear morphology of lesions in newborn $Rb^{-/-}p130^{-/-}LacZ$ chimeras resembled the inner rather than the outer nuclear layer (Fig. 5, panel II, F). Furthermore, in contrast to wild-type cells, which all had left the cell cycle by postnatal day 10 (Young 1985), $Rb^{-/-}p130^{-/-}$ cells in the lesions were actively synthesizing DNA as evidenced by BrdU incorporation (Fig. 5, panel II, E,F). These data indicate that only a subset of *Rbp130*-deficient retinoblasts committed to the inner nuclear layer can escape cell cycle control and form hyperplastic lesions, which are likely the precursors of retinoblastoma later in life.

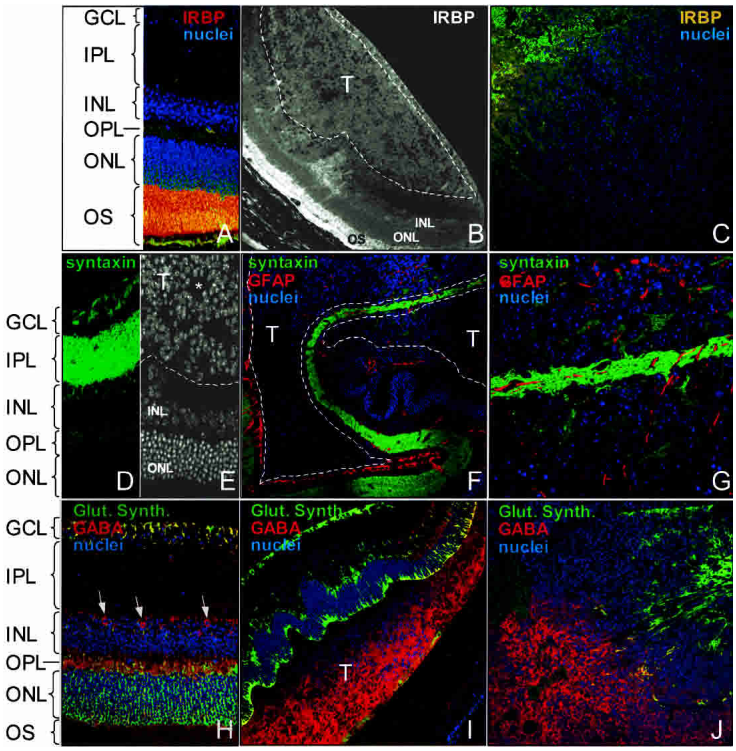

Figure 4. Inner nuclear layer characteristics of $Rb^{-/-}p130^{-/-}$ retinoblastomas. Immunohistochemical staining for retinal markers in a normal retina (*A*,*D*,*H*) and different $Rb^{-/-}p130^{-/-}$ retinoblastomas (*B*,*C*,*E–G*,*I*,*J*). (*A*) Normal retina showing IRBP in the outer segments (OS) of the photoreceptor cells. (*B*) IRBP staining was absent in retinoblastomas in a 1-mo-old (*B*) or a 3-mo-old (*C*) chimera. (*D*) Normal retina showing Syntaxin-positive amacrine cells in the inner nuclear layer (INL) and their synaptic processes in the inner plexiform layer. (*E*) Topro-3 DNA-stained tumor nuclei resemble the INL. A rosette-like structure is indicated with an asterisk. (*F*) Syntaxin+ as well as GFAP+ (Müller glia cells) cells were identified locally in retinoblastoma. (*G*) Syntaxin+ and GFAP+ cells in retinoblastoma close to remnants of amacrine synaptic processes. (*H*) Normal retina showing GABAergic amacrine cells in the INL (arrows) and Müller glia cells and their synaptic processes, identified by glutamine synthetase expression, in the GCL, INL, and ONL. (*I*) Extensive positive staining for GABA but not for glutamine synthethase in a retinoblastoma in a 1-mo-old chimera. (*J*) Local staining for GABA and glutamine synthetase in a retinoblastoma in a 3-mo-old chimera. (*B*,*E*,*F*) Tumor borders are indicated with dotted lines. Magnification: *A*,*D*,*E*,*H*, 20×; *B*,*C*,*F*,*I*,*J*, 10×; *G*, 40×.

Absence of pRb and p130 predisposes to pheochromocytoma and lung hyperplasia

Six out of 11 $Rb^{-/-}p130^{-/-}$ chimeras developed bilateral adrenal medullary tumors (Fig. 6A,B; Table 2), some already at 2 wk of age (Fig. 6C). The ES cell origin of these tumors was confirmed by PCR amplification of the D2Mit94 CA-repeat marker from tumor DNA (Fig. 3) and whole mount X-gal staining taking advantage of β-galactosidase-marked ES cells (Fig. 6F). Positive staining for the neuro-endocrine tissue markers chromogranin A and synapthophysin and negative staining for S-100 (Fig. 6D,E; data not shown), identified the tumors as pheochromocytomas (PCC) (Lloyd et al. 1985). The tumors were actively proliferating as evidenced by the presence of mitotic figures and incorporation of BrdU (Fig. 6G). The adrenal medulla of $Rb^{+/-}p130^{-/-}$ chimeric animals up to 9 mo of age did not display hyperplasia or tumors, despite the presence of ES-cell-derived cells (Fig. 6H). However, one out of 15 $Rb^{+/-}p130^{-/-}$ chimeric animals developed a unilateral ES-cell-derived PCC at 14 mo of age (Fig. 6I). Since $Rb^{-/-}$ chimeric mice showed hyperplastic nodules in the adrenal medulla, but never full blown tumors (Robanus Maandag et al. 1994; Williams et al. 1994a), we conclude that p130 suppresses oncogenic transformation of pRB-deficient adrenal medulla cells.

Histological examination of the lungs of $Rb^{-/-}p130^{-/-}$ chimeric mice showed that seven mice contained hyperplastic lesions in the bronchial epithelium (Fig. 7A–C) and, occasionally, in alveolar parts (Fig. 7B). All lesions were of ES-cell origin as evidenced by blue staining (Fig. 7E–G). The presence of blue patches in the epithelial lining of the bronchia that were histologically normal, suggests that inactivation of *Rb* and *p130* is not sufficient to induce bronchial hyperplasia (Fig. 7E). Consistently, we did not observe bronchial abnormalities in $Rb^{+/-}p130^{-/-}$ chimeric mice, although ES cell descendants were abundantly present (Fig. 7H). Positive staining for the neuro-endocrine-specific marker synaptophysin showed that all hyperplastic lesions were of

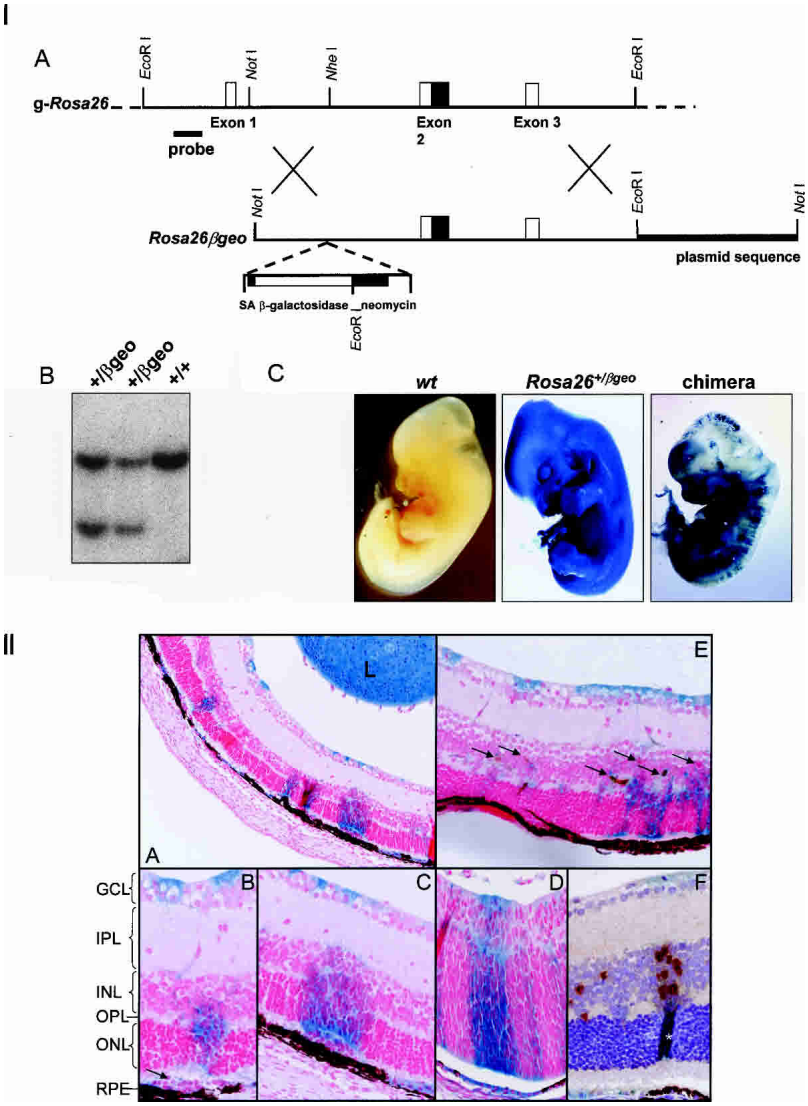

Figure 5. Early stages of retinoblastoma detected by using *LacZ*-tagged ES cells. (Panel *I*, *A*) The *Rosa26*–βgeo targeting construct. (*B*) Southern blot showing targeted *Rosa26* alleles. (*C*) *Rosa26*βgeo ES cells were used to generate $Rosa26^{+/\beta geo}$ embryos and mice. X-gal staining shows ubiquitous β-galactosidase expression in $Rosa26^{+/\beta geo}$ embryos. Chimeric embryos generated with *Rosa26*βgeo-tagged ES cells show patchy β-galactosidase staining. (Panel *II*) Histological sections of X-gal-stained eyes of two 2-wk-old $Rb^{-/-}p130^{-/-}$ chimeric mice, counterstained with nuclear fast red. (*A*) Overview of retina and lens (L) showing β-galactosidase-positive retinal cells. (*B*,*C*) ES cell-derived retinal lesions between the INL and ONL. Note the presence of β-galactosidase-positive cells also between the ONL and RPE (*B*; arrow). (*D*) Normal development of ES cell-derived retinal cells in the retina of an $Rb^{-/-}p130^{-/-}$ chimeric embryo 18 d p.c. (*E*) Proliferating cells in the INL part of β-galactosidase-positive retinal lesions (arrows) identified by anti-BrdU staining and nuclear fast red counterstaining. (*F*) Anti-BrdU and hematoxilyn-eosin-counterstained retinal lesion showing proliferating cells in the INL part of retinal lesions. The asterisk indicates a processing artifact. Magnification: *A*, 10×; *B–E*, 20×.

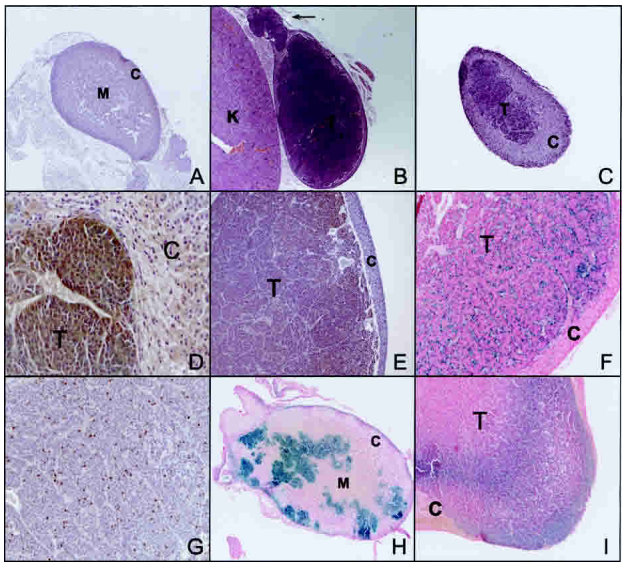

Figure 6. Neuro-endocrine adrenal medullary tumors in $Rb^{-/-}$ $p130^{-/-}$ chimeras. Hematoxylyn-eosin-stained (*A–E,G*) and X-gal-stained/nuclear fast red-counterstained (*F,H,I*) histological sections of adrenal gland and adrenal medullary tumors. (*A*) Normal adrenal gland in an $Rb^{-/-}p130^{-/-}$ chimeric mouse. (*B*) Large adrenal medullary tumor invading the retroperitoneal fat (arrow). (*C*) Small adrenal medullary gland tumor in a 2-wk-old chimera. (*D,E*) Adrenal medullary tumors stain positive for neuro-endocrine markers chromogranin A (*D*) and synaptophysin (*E*). (*F*) An X-gal-stained $Rb^{-/-}p130^{-/-}$ adrenal tumor, counterstained with nuclear fast red. In contrast to the adrenal cortex, the tumor entirely consists of β-galactosidase+ cells. (*G*) Extensive proliferation in an adrenal medullary tumor indicated by anti-BrdU staining. (*H*) No tumor development in the adrenal medulla of a 9-mo-old $Rb^{+/-}p130^{-/-}$ chimera despite the presence of β-galactosidase+ cells. (*I*) Unilateral adrenal medullary tumor in a 14-mo-old $Rb^{+/-}p130^{-/-}$ chimera showing β-galactosidase+ cells. (C) Adrenal cortex; (M) adrenal medulla; (T) tumor; (K) kidney. Magnification: *A,C,E,* 5×; *B,* 2.5×; *D,F,G,H,* 10×; *I,* 20×.

neuro-endocrine origin (Fig. 7I; Lauweryns et al. 1972). Therefore, these lesions are likely precursors of small cell lung cancer and identify p130 as a suppressor of this tumor type.

Discussion

Despite the central role of pRB in cell cycle control and human cancer, the tumor spectrum in pure $Rb^{+/-}$and chimeric $Rb^{-/-}$ mice is remarkably limited. Tumor development in these animals may be suppressed by the pRB homologs p107 or p130; however, embryonic or perinatal lethality associated with compound loss-of-function mutations of *Rb* family members has precluded assessing this hypothesis. We have therefore taken an alternative approach, i.e., combining loss-of-function mutations in chimeric mice generated from mutant ES cells. We realize this approach has some caveats. For example, the cohorts of chimeric mice show high variations in ES cell contribution precluding quantification of the latency and incidence of tumor development.

Nevertheless, this approach has identified p107 and p130 as genuine tumor suppressors in a number of tissues. Thus, p107 alone collaborates with pRb in suppressing development of coecal adenocarcinomas, osteosarcomas, lymphomsarcomas, leiomyosarcomas, and tumors located to the thyroid, adrenal gland, and ovary. Interestingly, osteosarcoma and leiomyosarcoma, are well-documented secondary malignancies in retinoblastoma patients (Moll et al. 1997; Ryan et al. 2003). p130 compensates for loss of pRb in suppressing pheochromocytomas and small cell lung cancer. Remarkably, p107 and p130 are both required to suppress transformation of pRb-deficient retinoblasts.

Tumor surveillance by the pRB protein family

One explanation for tumor development upon concomitant ablation of pRB and p107 or p130 may be derived from the critical role of pocket proteins in the $p19^{ARF}$–p53 tumor surveillance pathway (Sherr 1998). Our present and previous results show that in MEFs, concomitant ablation of *Rb* and *p107* or *Rb* and *p130* disabled the $p19^{ARF}$–p53 tumor surveillance mechanism causing immortality and allowing sustained proliferation upon expression of oncogenic Ras^{V12} (see also Dannenberg et al. 2000; Peeper et al. 2001). Consistently, development of

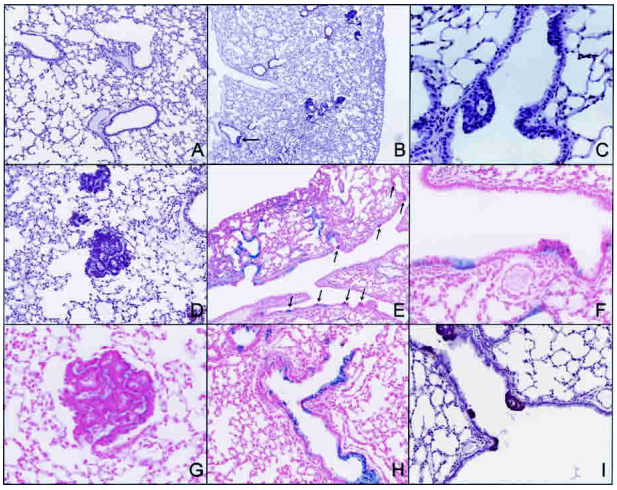

Figure 7. Pulmonary neuro-endocrine epithelial hyperplasia in $Rb^{-/-}p130^{-/-}$ chimeric mice. (*A*) Normal lung. (*B*) Alveolar hyperplastic nodules and bronchial epithelial hyperplasia (arrow) in a 5-mo-old $Rb^{-/-}p130^{-/-}$ chimera. (*C,D*) Bronchial epithelial hyperplasia in a 2.5-mo-old (*C*) and a 5-mo-old (*D*) $Rb^{-/-}p130^{-/-}$ chimera. (*E*) X-gal-stained/nuclear-fast-red-counterstained $Rb^{-/-}$ $p130^{-/-}$ chimeric lung, containing multiple bronchial epithelial hyperplasias (arrows). (*F,G*) Only β-galactosidase+ $Rb^{-/-}p130^{-/-}$ ES cell-derived cells are present in bronchial epithelial hyperplasias. (*H*) $Rb^{+/-}p130^{-/-}$ ES-cells contributed to the lung of a 9-mo-old $Rb^{+/-}p130^{-/-}$ chimeric mouse but did not form hyperplastic lesions. (*I*) Bronchial epithelial hyperplasia staining positive for the neuro-endocrine marker synapthophysin. Magnification: *A,D,H,* 20×; *B,E,* 10×; *C,G,* 40×; *F,I,* 20×.

retinoblastoma or PCC in pocket protein deficient mice did not require mutation of p53 (Supplementary Fig. 1). These results may suggest that in certain cell types $p19^{ARF}$–p53 and pocket proteins are part of the same tumor surveillance mechanism and that loss of this pathway contributes to tumor development.

It should be noted, however, that the tumor spectrum in *Rb/p107*- and *Rb/p130*-defective chimeras did not entirely overlap. Thus, the requirement for pocket proteins in tumor suppression is cell-type dependent. For example, in the retina, similar as in MEF cultures, p107 and p130 are *both* required to suppress proliferation of pRb-deficient cells, while in the adrenal gland p130 *alone* can compensate for loss of pRb. This may indicate that the suppression of tumorigenesis by p107 and p130 involves other, tissue-specific functions besides regulation of E2Fs. For example, the occurrence of osteosarcomas in $Rb^{+/-}p107^{-/-}$ chimeras but not in $Rb^{+/-}p130^{-/-}$ may be related to a specific role of p107 in bone development (Thomas et al. 2001; Laplantine et al. 2002).

Retinoblastoma origin

By LacZ tagging we showed that only a subset of $Rb^{-/-}p130^{-/-}$ retinoblasts, displaying features of inner nuclear layer nuclei, sustained continuous proliferation. Additionally, retinoblastomas in both $Rb^{-/-}p107^{-/-}$ and $Rb^{-/-}p130^{-/-}$ chimeras expressed amacrine-specific markers. Based on immunohistochemical analyses and morphological characteristics, human retinoblastoma was hypothesized to originate from photoreceptor cells in the outer nuclear layer (Bogenmann et al. 1988; Tajima et al. 1994). However, analyses of early, small retinoblastomas pointed to an inner nuclear layer origin, although they showed Flexner-Wintersteiner rosettes (Gallie et al. 1999). Thus, murine retinoblastomas resemble at least a subset of human retinoblastoma.

Similar findings were recently reported using heritable mouse models for retinoblastoma in which *Rb* was ablated in a *p107*- or *p130*-deficient background (Chen et al. 2004; MacPherson et al. 2004). Also in these models, amacrine cells were identified as the major component of retinoblastomas. These reports also showed that loss of *Rb* in the developing retina extended the proliferative capacity of all retinal precursors, which was exacerbated by concomitant loss of *p107*. Our results show that also combined loss of *Rb* and *p130* caused ectopic proliferation which, at day 14 after birth, was confined to the inner nuclear layer and caused severe dysplasia. As amacrine cells ultimately arrest, it was suggested that retinoblastoma in mice requires an extra genetic alteration that overcomes cell cycle arrest rather than apoptotic cell death (Chen et al. 2004). Enhanced proliferation of double knockout cells may facilitate the acquisition of such an alteration. Alternatively, conforming to our in vitro data, the delayed cell cycle exit of double knockout cells may indicate that oncogenic signals can induce a bypass of differentiation more easily in cells that lack both *Rb* and *p107* or *Rb* and *p130*. In cells lacking only *Rb* this would lead to p107- and p130-mediated cell cycle arrest.

Loss of p130 in adrenal gland and small cell lung cancer

While $Rb^{+/-}$ mice and $Rb^{-/-}$ chimeras display adrenal medulla hyperplasia (Robanus Maandag et al. 1994; Williams et al. 1994a; Yamasaki et al. 1998), $Rb^{-/-}p130^{-/-}$ chimeric mice developed ES cell-derived bilateral adrenal medullary tumors displaying characteristics of pheochromocytomas (PCC). $Rb^{+/-}p130^{-/-}$ chimeras developed the same tumors with a much longer latency, suggesting that loss of pRB is a rate-limiting step in the onset of this tumor type. In humans, this tumor of neuro-endocrine origin frequently shows loss of pRB expression (Gupta et al. 2000). Our observations indicate that also p130 plays a role in suppressing PCC.

Other neuro-endocrine cells that are affected by ablation of pRb and p130 are pulmonary neuro-endocrine epithelial cells. $Rb^{-/-}p130^{-/-}$ chimeric mice readily developed hyperplasia originating from this cell type. Although these hyperplastic lesions did not progress into full tumors before the appearance of other tumors, it is possible that they are precursors of small cell lung cancer. Small cell lung cancer (SCLC) in humans shows in more than 90% of the cases loss of heterozygosity (LOH) of chromosome region 13q14, harboring *RB*, and in more than 70% of the cases also LOH of the *p130* containing chromosome arm 16q (Stanton et al. 2000), suggesting that a large fraction of these tumors has lost both pRB and p130 expression. Furthermore, inactivating *p130* mutations were found in a pRB-deficient SCLC cell line (Helin et al. 1997) and in primary SCLCs (Claudio et al. 2000). In mice combined loss of pRb and p53 also resulted in bronchial epithelial hyperplasia and SCLC (Williams et al. 1994b; Meuwissen et al. 2003). Together with our data, this may again suggest that p53 and p130 act in a similar tumor suppression pathway. Analysis of mice with conditional inactivation of *Rb* and *p130* in the bronchial epithelium will be required to determine whether loss of p130 can indeed substitute for loss of p53 in development of SCLC.

Materials and methods

Generation of Rb *gene family mutant ES cells, chimeras and MEFs*

Knockout alleles of *Rb*, *p107* and *p130* were generated in 129OLA (E14) embryonic stem cells as described (te Riele et al. 1992; Robanus-Maandag et al. 1998; Dannenberg et al. 2000). The *Rosa26*βgeo targeting construct was generated by inserting a splice-acceptor-site–β-geo fragment from plasmid pβgeo, into a NheI site of a 10-kb genomic *Rosa26* DNA fragment (Friedrich and Soriano 1991). Genomic DNA isolated from G418 resistant colonies was digested with EcoRI and subjected to Southern blot analysis, using a 5′ external PstI–SalI 800 base pair *Rosa26* genomic probe to identify correctly targeted clones. These were obtained with a frequency of 97%. Chimeras were generated by

injecting mutant ES cells into C57Bl/6 blastocysts. The derivation of MEF cultures from chimeric embryos and the 3T9 protocol are described in Dannenberg et al. (2000).

Virus production and infection of MEFs

Ecotropic retroviral supernatants were produced by transfecting 293T (Phoenix) packaging cells with 50 µg viral DNA using calcium-phosphate precipitation. The medium was collected and filtered through a 0.45-µm filter 48, 56, and 72 h post-transfection. Low-density cultures of MEFs were infected at least three times for 3 h with viral supernatant containing 4 µg/mL polybrene (Sigma) yielding infection efficiencies of 95% or more. After the last infection, the viral supernatant was exchanged for fresh medium and the cells were allowed to recover for 48 h.

Protein analyses

Protein levels were determined by Western blot analyses following established protocols. Antibodies against p107 (C-18), p130 (C-20), CDK4 (C-22), Cyclin E, (M-20), Cyclin A, E2F-1 (C-20), $p21^{CIP}$ (C-19), were obtained from Santa Cruz; the pRB antibody (G3-245) from BD Pharmingen; RAS (R02120) and DHFR antibodies from BD Transduction Laboratories; the $p19^{ARF}$ antibody (R562) from Abcam; the p53 antibody (Ab-7) from Oncogene Science. Peroxidase conjugated goat anti-rabbit and goat anti-mouse secondary antibodies were from Biosource. To detect p53 antibodies we used peroxidase conjugated rabbit anti-goat antibodies from DAKO.

Southern Blot analysis of tumor DNA

Tumors were minced and incubated overnight in 50 mM Tris (pH 8.5), 1 mM EDTA, 0.5% Tween-20, and 200 µg/mL proteinase K at 55°C. DNA was extracted using iso-propanol precipitation. To identify the ES cell- and blastocyst-derived wild-type *Rb* alleles and the *Rb* knockout allele, 10 µg of genomic DNA was digested with StuI and analyzed by Southern blotting using a 5′ external probe (te Riele et al. 1992).

Isolation of DNA from paraffin-embedded tumors and PCR analysis

Tumor tissue was removed from deparaffinized unstained paraffin sections using a laser capture microscope. Tumor samples were incubated overnight in 20 µL of 50 mM KCl, 10 mM Tris (pH 8), 2.5 mM $MgCl_2$, 0.1 mg/mL gelatin, 0.46% Tween-80, 0.1 mg/mL proteinase K at 37°C. To inactivate proteinase K, samples were incubated at 80°C for 10 min and subsequently centrifuged at 14,000 K for 5 min. Five microliters of the DNA solution was used in a PCR using D2mit94 5′ FAM labeled primer set (Mouse MapPairs, Research Genetics). PCR products were separated on an ABI Prism 3700 DNA Analyzer.

X-gal staining

Tissues and embryos were fixed in freshly made 0.1 M sodium phosphate (pH 7.3), 1.5% formaldehyde, 0.2% glutaraldehyde, 2 mM $MgCl_2$, and 5 mM EGTA for 30–90 min. The samples were rinsed for 3 × 10 min in 0.1 M sodium phosphate (pH 7.3), 0.1% sodium deoxycholate 0.2% NP40, 2 mM $MgCl_2$. Staining with X-gal (1 mg/mL; Roche) was performed in the rinse buffer containing 5 mM K_3FeCN and 5 mM K_4FeCN and 0.2 mM Tris (pH 7.5) overnight at room temperature. After an additional 6 h of staining in fresh solution, samples were rinsed 3 × 10 min, fixed overnight in 4% phosphate buffered formalin, and processed for paraffin embedding. Four-micrometer sections were stained either with hematoxylin or nuclear fast red.

BrdU/FUdr labeling, histology and immunohistochemistry

Mice received an i.p. injection of 5-bromo-2′-deoxyuridine (BrdU; Sigma) and 5-fluoro-2′-deoxyuridine (FUdr; Sigma) in PBS (50 and 10 mg/kg body weight) 2 h before being sacrificed. Tissues were processed for X-gal staining or directly fixed in phosphate-buffered formalin. Five-micron sections of paraffin embedded tissues were stained with hematoxilyn and eosin. For immunohistochemistry, sections were dehydrated, heated for 15 min in a citrate buffer (pH 6.0) using a microwave for antigen retrieval, and blocked in 1% normal goat serum at room temperature. Antibodies detecting BrdU (DAKO), Chromogranin A (Chemicon), GABA (Sigma), GFAP (Chemicon), glutamine synthetase (BD Transduction Laboratories), IRBP (gift of Y. De Kozak, U450 INSERM, Paris, France), p53 (pAb421; Oncogene Science), p75 (Chemicon), synapthophysin (Chemicon), and syntaxin (HPC-1; Sigma) were diluted in 1% normal goat serum. Goat anti-mouse (Alexa 488) and goat anti-rabbit (Alexa 568) antibodies were obtained from Molecular Probes. Nuclear staining was performed using Topro-3 stain diluted 1:1000 in mounting medium (Vectashield).

Acknowledgments

We thank Elly van Riet for technical assistance; Tanja Hetem-Maidment, Sjaak Greven, Muriël Lageweg-Beumkes, and Auke Zwerver for animal care; Kees de Goeij, Cedric Boersema, Jurjen Bulthuis, and Marlon Tjin-A-Koeng for immunohistotechnical assistance; Lauran Oomen and Leny Brocks for help with confocal laser and digital light microscopy; Jeroen Poodt and Lucie Boerrigter-Barendsen for help with the laser capture microscopy; Roelof Pruntel for PCR product analysis; Dr. Philippe Soriano for providing *Rosa26* genomic DNA and the pβgeo plasmid; and Floris Foijer and Jacob Bo Hansen for critically reviewing this manuscript. This work was supported by The Netherlands Cancer Foundation through project grants NKI 95-956 and NKI 2000-2232 to H.t.R (J.-H.D., L.S.).

References

Barnstable, C.J., Hofstein, R., and Akagawa, K. 1985. A marker of early amacrine cell development in rat retina. *Brain Res.* **20:** 286–290.

Beijersbergen, R.L., Carlée, L., Kerkhoven, R.M., and Bernards, R. 1995. Regulation of the retinoblastoma protein-related p107 by G1 cyclin complexes. *Genes & Dev.* **9:** 1340–1353.

Bjorklund, H., Bignami, A., and Dahl, D. 1985. Immunohistochemical demonstration of glial fibrillary acidic protein in normal rat Müller glia and retinal astrocytes. *Neurosci. Lett.* **54:** 363–368.

Bogenmann, E., Lochrie, M.A., and Simon, M.I. 1988. Cone cell-specific gene expressed in retinoblastoma. *Science* **240:** 76–78.

Bookstein, R., Rio, P., Madreperla, S.A., Hong, F., Alfred, C., Grizzle, W.E., and Lee, W.H. 1990. Promoter deletion and loss of retinoblastoma gene expression in human prostate carcinoma. *Proc. Natl. Acad. Sci.* **87:** 7762–7766.

Bremner, R., Cohen, B.L., Sopta, M., Hamel, P.A., Ingles, C.J., Gallie, B.L., and Phillips, R.A. 1995. Direct transcriptional repression by pRB and its reversal by specific cyclins. *Mol. Cell. Biol.* **15:** 3256–3265.

Canhoto, A.J., Chestukhin, A., Litovchick, L., and DeCaprio,

J.A. 2000. Phosphorylation of the retinoblastoma-related protein p130 in growth-arrested cells. *Oncogene* **19:** 5116–5122.

Chen, D., Livne-bar, I., Vanderluit, J.L., Slack, R.S., Agochiya, M., and Bremner R. 2004. Cell-specific effects of RB or RB/p107 loss on retinal development implicate an intrinsically death-resistant cell-of-origin in retinoblastoma. *Cancer Cell* **5:** 539–551.

Chow, K.N. and Dean, D.C. 1996. Domains A and B in the Rb pocket interact to form a transcriptional repressor motif. *Mol. Cell. Biol.* **16:** 4862–4868.

Clarke, A.R., Robanus Maandag, E., Van Roon, M., Van der Lugt, N.M.T., Van der Valk, M., Hooper, M.L., Berns, A., and Te Riele, H. 1992. Requirement for a functional Rb-1 gene in murine development. *Nature* **359:** 328–330.

Claudio, P.P., Howard, C.M., Baldi, A., De Luca, A., Fu, Y., Condorelli, G., Sun, Y., Colburn, N., Calabretta, B., and Giordano, A. 1994. p130/RB2 has growth suppressive properties similar to yet distinctive from those of retinoblastoma family members pRB and p107. *Cancer Res.* **54:** 5556–5560.

Claudio, P.P., Howard, C.M., Pacilio, C., Cinti, C., Romano, G., Minimo, C., Maraldi, N.M., Minna, J. D., Gelbert, L., Leoncini, L., et al. 2000. Mutations in the retinoblastoma-related gene *RB2/p130* in lung tumors and suppression of tumor growth in vivo by retrovirus-mediated gene transfer. *Cancer Res.* **6:** 372–382.

Cobrinik, D., Lee, M.-H., Hannon, G., Mulligan, G., Bronson, R.T., Dyson, N., Harlow, E., Beach, D., Weinberg, R.A., and Jacks, T. 1996. Shared role of the pRB-related p130 and p107 proteins in limb development. *Genes & Dev.* **10:** 1633–1644.

Dannenberg, J.-H., Rossum, A. van, Schuijff, L., and te Riele, H. 2000. Ablation of the retinoblastoma gene family deregulates G_1 control causing immortalization and increased cell turnover under growth restricting conditions. *Genes & Dev.* **14:** 3051–3064.

Dyson, N. 1998. The regulation of E2F by pRB-family proteins. *Genes & Dev.* **12:** 2245–2262.

Eisenfield, A.J., Bunt-Milam, A.H., and Sarthy, P.V. 1984. Müller cell expression of glial fibrillary acidic protein after genetic and experimental photoreceptor degeneration in the rat retina. *Invest. Ophthalmol. Vis. Sci.* **25:** 1321–1328.

Ewen, M.E., Xing, Y.G., Lawrence, J.B., and Livingston, D.M. 1991. Molecular cloning, chromosomal mapping, and expression of the cDNA for p107, a retinoblastoma gene product-related protein. *Cell* **66:** 1155–1164.

Friedrich, G. and Soriano, P. 1991. Promoter traps in embryonic stem cells: A genetic screen to identify and mutate developmental genes in mice. *Genes & Dev.* **5:** 1513–1523.

Friend, S.H., Bernards, R., Rogelj, S. Weinberg, R.A., Rapaport, J.M., Albert, D.M., and Drya, T.P. 1986. A human DNA segment with properties of the gene that predisposes to retinoblastoma and osteosarcoma. *Nature* **323:** 643–646.

Friend, S.H., Horowitz, J.M., Gerber, M.R., Wang, X.F., Bogenmann, E., Lif, P., and Weinberg, R.A. 1987. Deletion of a DNA sequence in retinoblastomas and mesenchymal tumours: Organization of the sequence and its encoded protein. *Proc. Natl. Acad. Sci.* **84:** 9059–9063.

Gallie, B.L., Campbell, C., Devlin, H., Duckett, A., and Squire, J.A. 1999. Developmental basis of retinal-specific induction of cancer by RB mutation. *Cancer. Res. (Suppl.)* **59:** 1731s–1735s.

Graña, X., Garriga, J., and Mayol, X. 1998. Role of the retinoblastoma protein family, pRB, p107 and p130 in the negative control of cell growth. *Oncogene* **17:** 3365–3383.

Gupta, D., Shidham, V., Holden, J., and Layfield, L. 2000. Prognostic value of immunohistochemical expression of topoisomerase α II, MIB-1, p53, E-cadherin, retinoblastoma gene protein product and HER-2/neu in adrenal and extra-adrenal pheochromocytomas. *Appl. Immunohistochem. Mol. Morphol.* **8:** 267–274.

Hannon, G.J., Demetrick, D., and Beach, D. 1993. Isolation of the Rb-related p130 through its interaction with CDK2 and cyclins. *Genes & Dev.* **7:** 2378–2391.

Hansen, K., Farkas, T., Lukas, J., Holm, K., Rönnstrand B., and Bartek, J. 2001. Phosphorylation-dependent and -independent functions of p130 cooperate to evoke a sustained G_1 block. *EMBO J.* **20:** 422–432.

Harbour, J.W. and Dean, D.C. 2000. The Rb/E2F pathway: Expanding roles and emerging paradigms. *Genes & Dev.* **14:** 2393–2409.

Harbour, J.W., Lai, S.-L., Whang-Peng, J., Gazdar, A.F., Minna, J.D., and Kaye, F.J. 1988. Abnormalities in structure and expression of the human retinoblastoma gene in SCLC. *Science* **241:** 353–357.

Haverkamp, S. and Wässle, H. 2000. Immunocytochemical analysis of the mouse retina. *J. Comp. Neurol.* **424:** 1–23.

Helin, K., Holm, K., Niebuhr, A., Eiberg, H., Tommerup, N., Hougaard, S., Poulsen, H.S., Spang-Thomsen, M., and Norgaard, P. 1997. Loss of the retinoblastoma protein-related p130 protein in small cell lung carcinoma. *Proc. Natl. Acad. Sci.* **94:** 6933–6938.

Hurford, R.K., Cobrinik, D., Lee, M.-H., and Dyson, N. 1997. pRB and p107/p130 are required for the regulated expression of different sets of E2F responsive genes. *Genes & Dev.* **11:** 1447–1463.

Ishida, S., Huang, E., Zuzan, H., Spang, R., Leone, G., West, M., and Nevins, J.R. 2001. Role for E2F in control of both DNA replication and mitotic functions as revealed from DNA microarray analysis. *Mol. Cell. Biol.* **21:** 4684–4699.

Jacks, T., Fazeli, A., Schmitt, E.M., Bronson, R.T., Goodell, M.A., and Weinberg, R.A. 1992. Effects of an Rb mutation in the mouse. *Nature* **359:** 295–300.

Kalma, Y., Marash, L., Lamed, Y., and Ginsberg, D. 2001. Expression analysis using DNA microarrays demonstrates that E2F-1 up-regulates expression of DNA replication genes including replication protein A2. *Oncogene* **20:** 1379–1387.

Laplantine, E., Rossi, F., Sahni, M., Basilico, C., and Cobrinik, D. 2002. FGF signaling targets the pRb-related p107 and p130 proteins to induce chondrocyte growth arrest. *J. Cell. Biol.* **158:** 741–750.

Lauweryns, J.M., Cokelaere, M., and Theunynck, P. 1972. Neuroepithelial bodies in the respiratory mucosa of various mammals: A light optical, ultrastructural and histochemical investigation. *Z. Zellforsch. Mikrosk. Anat.* **135:** 569–592.

Lee, E.Y.-H.P., To, H., Shew, J.-Y., Bookstein, R., Scully, P., and Lee, W.-H. 1988. Inactivation of the retinoblastoma susceptibility gene in human breast cancers. *Science* **241:** 218–221.

Lee, E.Y.-H.P., Chang, C.-Y., Hu, N., Wang, Y.-C., Lai, C.-C., Herrup, K., Lee, W.-H., and Bradley, A. 1992. Mice deficient for *Rb* are nonviable and show defects in neurogenesis and haematopoiesis. *Nature* **359:** 288–294.

Lee, M.-H., Williams, B.O., Mulligan, G., Mukai, S., Bronson, R.T., Dyson, N., Harlow, E., and Jacks, T. 1996. Targeted disruption of *p107*: Functional overlap between *p107* and *Rb*. *Genes & Dev.* **10:** 1621–1632.

Li, Y., Graham, C., Lacy, S., Duncan, A.M.V., and Whyte, P. 1993. The adenovirus E1A-associated 130-kD protein is en-

coded by a member of the retinoblastoma gne family and physically interacts with cyclins A and E. *Genes & Dev.* **7:** 2366–2377.

Lloyd, R.V., Blaivas, M., and Wilson, B.S. 1985. Distribution of chromogranin and S100 protein in normal and abnormal adrenal medullary tissues. *Arch. Pathol. Lab. Med.* **109:** 633–635.

Lundberg, A.S. and Weinberg, R.A. 1998. Functional inactivation of the retinoblastoma protein requires sequential modification by at least two distinct cylin–cdk complexes. *Mol. Cell. Biol.* **18:** 753–761.

MacPherson, D., Sage, J., Kim, T., Ho, D., McLaughlin, M.E., and Jacks, T. 2004. Cell type-specific effects of *Rb* deletion in the murine retina. *Genes & Dev.* **18:** 1681–1694.

Meuwissen, R., Linn, S.C., Linnoila, R.I., Zevenhoven, J., Mooi, W.J., and Berns, A. 2003. Induction of small cell lung cancer by somatic inactivation of both Trp53 and Rb1 in a conditional mouse model. *Cancer Cell* **4:** 181–189.

Moll, A.C., Imhof, S.M., Bouter, L.M., and Tan, K.E. 1997. Second primary tumors in patients with retinoblastoma. A review of the literature. *Opthalmic Genet.* **1:** 27–34.

Muller, H., Bracken, A.P., Vernell, R., Moroni, M.C., Christians, F., Grassili, E., Prosperini, E., Vigo, E., Oliner, J.D., and Helin, K. 2001. E2Fs regulate the expression of genes involved in differentiation, development, proliferation and apoptosis. *Genes & Dev.* **15:** 267–285.

Peeper, D.S., Dannenberg, J.-H., Douma, S., te Riele, H., and Bernards, R. 2001. Escape from premature senescence is not sufficient for oncogenic transformation. *Nat. Cell Biol.* **3:** 198–302.

Rayman, J.B., Takahashi, Y., Indjeian, V.B., Dannenberg, J.-H., Catchpole, S., Watson, R.J., te Riele, H., and Dynlacht, B.D. 2002. E2F mediates cell cycle-dependent transcriptional repression in vivo by recruitment of an HDAC1/mSin3B corepressor complex. *Genes & Dev.* **16:** 933–947.

Ren, B., Cam, H., Takahashi, Y., Volkert, T., Terragni, J., Young, R.A., and Dynlacht, D. 2002. E2F integrates cell cycle progression with DNA repair, replication, and G_2/M checkpoints. *Genes & Dev.* **16:** 245–256.

Robanus Maandag, E.C., Van der Valk, M., Vlaar, M., Feltkamp, C., O'Brien, J., Van Roon, M., Van der Lugt, N., Berns, A., and te Riele, H. 1994. Developmental rescue of an embryonic-lethal mutation in the retinoblastoma gene in chimeric mice. *EMBO J.* **13:** 4260–4268.

Robanus-Maandag, E., Dekker, M., Van der Valk, M., Carrozza, M.-L., Jeanny, J.-C., Dannenberg, J.-H., Berns, A., and te Riele, H. 1998. p107 is a suppressor of retinoblastoma development in pRb-deficient mice. *Genes & Dev.* **12:** 1599–1609.

Ruas, M. and Peters, G. 1998. The $p16^{INK4a}$/CDKN2A tumor suppressor and its relatives. *Biochem. Biophys. Acta Rev. Cancer* **1378:** F115–F177.

Ryan, R.S., Gee, R., O'Connell, J.X., Harris, A.C., and Munk, P.L. 2003. Leiomyosarcoma of the distal femur in a patient with a history of bilateral retinoblastoma: A case report and review of the literature. *Skeletal Radiol.* **32:** 476–480.

Sage, J., Mulligan, G.J., Attardi, L.D., Miller, A., Chen, S., Williams, B., Theorou, E., and Jacks, T. 2000. Targeted disruption of the three Rb-related genes leads to loss of G1 control and immortalization. *Genes & Dev.* **14:** 3037–3050.

Sherr, C.J. 1996. Cancer cell cycles. *Science* **274:** 1672–1677.

——. 1998. Tumor surveillance by the ARF–p53 pathway. *Genes & Dev.* **12:** 2984–2991.

——. 2001. The Ink4a/ARF network in tumour suppression. *Nat. Rev. Mol. Biol.* **2:** 731–737.

Sherr, C.J. and Roberts, J.M. 1999. CDK inhibitors: Positive and negative regulators of G1-phase progression. *Genes & Dev.* **13:** 1501–1512.

Stanton, S.E., Shin, S.W., Johnson, B.E., and Meyerson, M. 2000. Recurrent allelic deletions of chromosome arms 15q and 16q in human small cell lung carcinomas. *Genes Chromosomes Cancer* **27:** 323–331.

Starostik, P., Chow, K.N., and Dean, D.C. 1996. Transcriptional repression and growth suppression by the p107 pocket protein. *Mol. Cell. Biol.* **16:** 3606–3614.

Tajima, Y., Munakata, S., Ishida, Y., Nakajima, T., Sugano, I., Nagao, K., Minoa, K., and Kondo, Y. 1994. Photoreceptor differentiation of retinoblastoma: An electron microscopic study of 29 retinoblastomas. *Pathol. Int.* **44:** 837–843.

T'Ang, A., Varley, J.M., Chakraborty, S., Murphree, A.L., and Fung, Y.K. 1988. Structural rearrangement of the retinoblastoma gene in human breast carcinoma. *Science* **242:** 263–266.

te Riele, H., Robanus Maandag, E., and Berns, A. 1992. Highly efficient gene targeting in embryonic stem cells through homologous recombination with isogenic DNA constructs. *Proc. Natl. Acad. Sci.* **89:** 5128–5132.

Thomas, D.M., Carty, S.A., Piscopo, D.M., Lee, J.S., Wang, W.F., Forrester, W.C., and Hinds, P.W. 2001. The retinoblastoma protein acts as a transcriptional coactivator required for osteogenic differentiation. *Mol. Cell* **2:** 303–316.

Trimarchi, J.M. and Lees, J.A. 2002. Sibling rivalry in the E2F family. *Nat. Rev. Mol. Cell. Biol.* **3:** 11–20.

Williams, B.O., Schmitt, E.M., Remington, L., Bronson, R.T., and Jacks, T. 1994a. Extensive contribution of *Rb*-deficient cell to adult chimeric mice with limited histopathological consequences. *EMBO J.* **13:** 4251–4259.

Williams, B.O., Remington, L., Albert, D.M., Mukai, S., Bronson, R.T., and Jacks, T. 1994b. Cooperative tumorigenic effects of germline mutations in Rb and p53. *Nat. Genet.* **74:** 480–484.

Wu, L., de Bruin, A., Saavedra, H.I., Starovic, M., Trimboli, A., Yang, Y., Opavska, J., Wilson, P., Thompson, J.C., Ostrowski, M.C., et al. 2003. Extra-embryonic function of Rb is essential for embryonic development and viability. *Nature* **421:** 942–947.

Yamasaki, L., Bronson, R., Williams, B.O., Dyson, N.J., Harlow, E., and Jacks, T. 1998. Loss of E2F-1 reduces tumorigenesis and extends the lifespan of $Rb^{+/-}$ mice. *Nat. Genetics* **18:** 360–364.

Young, R.W. 1985. Cell differentiation in the retina of the mouse. *Anat. Rec.* **212:** 199–205.

Zamanian, M. and La, T.N. 1993. Transcriptional repression by the Rb-related protein p107. *Mol. Biol. Cell* **4:** 389–396.

Zhu, L., van den Heuvel, S., Helin, K., Fattaey, A., Ewen, M., Livingston, D., Dyson, N., and Harlow, E. 1993. Inhibition of cell proliferation by p107, a relative of the retinoblastoma protein. *Genes & Dev.* **7:** 1111–1125.